V. Epshteyn (ITEP) ATLAS-FCAL beam tests 2003 Internal Note 5, 2003-12-21
12-22/01/2004, with P. Gorbunov (U. of Toronto & ITEP)

A study of non-linear effects in FCAL pulser calibration data

1. Introduction

In the analysis by J.Rutherfoord and A.Savin [Ref.1] a strong non-linearity of the FEB response to calibration pulser signals was observed, in the measurement with the signal cables disconnected from the FEC baseplane (Fig.1,2). It was indicated that the effect is present in the medium gain data and is less pronounced for high gain.

In this note an attempt is made to interpret this phenomenon in terms of a behavior of FEB amplifiers in the very high-frequency domain associated with the fast rise-time of the FCAL pulser signals. The analog channel (pulser / baseplane / FEB input tracks / preamplifier / shaper) is simulated with `PSpice`, using the published information on the design of these parts [Ref.2]. A good qualitative agreement with data is obtained. At the same time, a lack of (or a controversial) information about the actual components and circuits used in the 2003 tests prevents from obtaining a perfect numerical agreement with data, in particular – describing a marked difference in non-linear behaviors of different FEBs.

In Section 2 the details of the analysis are given and the observations are summarized. Section 3 contains a qualitative discussion, introduces a simulation model of the FEB analogue part and presents the results. Section 4 contains concluding remarks, in particular – comments on the technical origin of the observed non-linearity.

2. Observations: calibration signal shapes and the non-linearity

The "long calibration" runs used for the analysis [Ref.3] correspond to 21 linearity scans with the calorimeter signal cables connected and 21 scans with the cables disconnected. We shall further refer to these data sets as **"*cables on*"** and **"*cables off*"**, respectively.

2.1 Signal shape and pedestals

For each FEB channel, a *raw waveform* for a given DAC value is obtained by averaging the ADC values over all 21 measurements, at each delay point. Thus, there are192=24×8 points in each waveform (where 24 is the number of samples and 8 – the number of different delays). After subtracting the *pedestal waveform* (see below), the average signal waveform is reconstructed by a least-square fit of the measurements with cubic splines. The *signal amplitude* is defined as the maximum of the fitted curve. This notation is used throughout the text, i.e. "a signal amplitude" means a *reconstructed amplitude*.

A non-zero signal is present on the shaper output even with DAC=0, due to transient processes in the pulser switches (Fig. 3). At the first moment of the calibration signal formation, a short (~1 ns) negative spike appears on the pulser output bus. Its duration and amplitude are defined by the duration of transient processes and the value of parasitic capacitances of the switches – essentially, by parameters of transistors. Since this spike is much shorter than the characteristic time constant of the shaper, the corresponding shaper output signal is close to the shaper's impulse response function. This component of the calibration signal represents a pedestal waveform for the signals with non-zero DAC, and has to be subtracted from the raw waveforms.[1] The "DAC=0" issue is discussed in the pulser design paper [Ref.2a, section 4. 1.1] and in our separate note [Ref.. 5] where the pulser model is confronted with data.

[1] The shape and amplitude of the pedestal waveform (after shaper) is weakly dependent on the switch current, but at low DAC values, where this effect really matters, it can be regarded as constant. A presence of a residual switch current at DAC=0 is an important factor affecting the pedestal signal shape [Ref . 5].

2.2 A glance at reconstructed calibration signals

Fig. 4 shows the reconstructed calibration pulse amplitudes for all channels, at DAC=750, with medium gain. This plot gives a general idea on the values and their uniformity. One channel (FEB4, input 44) appears to have a missing or broken 695Ω resistor on the base-plane. The calibration signal in that channel passes through a tiny parasitic capacitance parallel to the missing resistor, and gets differentiated. This gives a chance to evaluate this parasitic capacitance, by a comparison with a normal calibration pulse shape (Fig. 5). The calculation yields 0.5 pF.

Fig. 6 shows an example of linearity scans over the entire DAC range (input 0, medium gain).

2.3 A non-linearity

An integral non-linearity (INL) is defined as a deviation of the measured response from a straight line drawn through the end-points (DAC=0 and DAC_{MAX}) of a DAC-scan graph:

$$nonlin_A = A - A_{LIN}, \quad A_{LIN} = DAC\frac{A(DAC_{MAX})}{DAC_{MAX}}, \quad nonlin_R = \frac{nonlin_A}{A_{LIN}}, \text{ where}$$

A is the signal amplitude for a given DAC value, DAC_{MAX} =1000 for the high gain and =4000 for the medium gain.

Fig. 7 shows an example of $nonlin_A$, as function of the signal amplitude, for input channel 0 and cables ***on***|***off***. The non-linearity observed with cables ***on*** never exceeds one half of an ADC channel (at medium gain), while with cables ***off*** it can reach 40 ADC channels, for the signal amplitude of about 500. The data processing is the same in both cases. Thus, a significant difference between ***on*** and ***off*** is seen. Another important observation is a big scatter (almost factor 3) of the INL values in different FEBs. A relative INL, $nonlin_R$, is a more convenient measure of the effect, see Fig. 8. We see that the non-linearity can exceed 10%.

Fig. 9 shows $nonlin_R$ as function of the input channel number for DAC=750, medium gain and input cables ***on*** and ***off***. The non-linearity seems to be smaller in the middle FEBs (3, 4 and 5) than in the FEBs 0-2 and 6, 7. The average $nonlin_R$ varies between different FEBs by more than factor 2.

By examining Figures 9 and 10, we notice a correlation between the response to DAC=4000 and the magnitude of the non-linearity in the same input channel, with cables ***off***. With cables ***on*** (Fig. 11), the response variations at high DAC are practically absent, therefore their appearance seem to be almost entirely due to the nonlinearity.

A prominent feature revealed by Fig 9 is a periodic structure in $nonlin_R$ plotted as function of the input channel. It is observed both for cables ***off*** and ***on***. The structure period corresponds to one FEB or, as Figure 12 shows, rather to one half of a FEB. Further insight is given by Figure 13 in which $nonlin_R$ is plotted as function of a sequential word number in the FEB ADC "super-record" ([Ref .3], Section 3.1). A period of 8 words is clearly seen. As [Ref .3] explains, every 16 successive words in a "super-record" correspond to 16 different ADCs, from 0 to 15. Thus, the non-linearity is clearly related to the FEB slice served by one ADC. What makes one such slice different from another? According to the FEB PCB layout [Ref. 2c], the main difference is in the PCB tracks connecting the input connector pin to the corresponding pre-amplifier input. Eight ADC slices located in one half of the FEB have different layouts and lengths of input tracks; this pattern is more or less reproduced in the second half of the FEB.

Note, that Figures 13 and 12 show the same effect because every eight successive input pins are connected to (different channels of) the same ADC: pins 0-7 –to ADC0, pins 8-15 –to ADC1 etc. The

structure seen in Figure 12 is, in fact, repeated 8 times (8 ADC channels) in Fig 13.[2]

A non-linearity is also observed in high-gain data (Fig. 15), but its magnitude is much smaller because the DAC range here is only 0-1000, while our measure of INL is roughly proportional to $DAC_{MAX.}$[3]

Let us summarize the observations. The observed non-linearity…

- is practically absent with the input cables ***on***, and appears with the cables ***off***;
- can be up to 12% at DAC=750, with medium gain;
- depends on the FEB, being minimal for the FEBs located in the middle of the crate and maximal for the FEBs which are closer either to the pulser board, or to the opposite end of the baseplane;
- has a periodic structure associated with the ADC number. The period of 8 seems to correspond to 8 different layouts of the conducting tracks connecting the pre-amplifiers to the input pins). This gives an important hint on the origin of the non-linearity.

3. An attempt to explain the observed non-linearity

3.1 Qualitative considerations

- The amplitude of a signal on the output of the pre-amplifier is:

$$A = Ical \cdot G_{TOT}, \quad G_{TOT} = kZ \cdot G_I, \quad kZ = \frac{Z_C}{Z_{IN} + Z_C},$$

Ical – the value is defined by the Injection R (695Ω) in Fig. 1;
G_I – pre-amplifier gain;
Z_{IN} – input impedance of the pre-amplifier;
Z_C – the impedance of the signal cables.

For cables ***on:*** $Z_C \approx Z_{IN}$, kZ≈1/2; for cables ***off:*** $Z_C = \infty$, kZ ≈ 1.

- When the cables are disconnected, the signal amplitude is doubled, but by itself this cannot cause a non-linearity (indeed, it is not seen with the cables ***on***, in a wide input signal range). Therefore, the only viable explanation is the amplitude dependence of G_I and Z_{IN}. The pre-amplifier gain does have a non-linearity dependent on the input signal amplitude – we see it in the case of cables ***off***. The input impedance also has a non-linearity of the same sign (in our pre-amplifiers Z_{IN} and G_I are correlated). With the cables ***on***, these two factors partially cancel each other and the overall non-linearity is small.

- If some part of the pre-amplifier is responsible for the non-linearity, its magnitude can fluctuate due to small variations of the component parameters in this part. However, the component parameter fluctuations are random, while we observe a clear relationship between $nonlin_R$ and the pre-amplifier location. The latter defines the layout and length of connecting PCB tracks (on the baseplane – between the pulser and the FEB input pin; on the FEB – between the input pin and the pre-amplifier hybrid), and the values of parasitic capacitances, for example the one which is parallel to the "Injection R" resistor (Fig. 1). The influence of these factors can only manifest itself at very high frequencies. This means that <u>the observed effects are related to the high-frequency part of the spectrum of the pulser signal or, in other words, to its very short rise-time.</u>

---

[2] The shapes look differently, because the order of ADCs in data is different from the order of ADCs on the board.
[3] In a simplest non-linear model Y=X(1+αX), the maximal value of $|\Delta Y/Y| = |\alpha|(X_{MAX}-X)/(1+\alpha X)$ is $|\alpha|X_{MAX}$ (at X=0).

- The non-linearity can be particularly pronounced with the cables ***off***, because a) the gain non-linearity is not partially compensated by the input impedance non-linearity and b) possible transients associated with reactive elements on the pre-amplifier input are not damped by the input cable.

- Thus, we have an acceptable qualitative "theory" for the non-linearity problems. In the next sub-section a simulation model supporting this theory is presented.

- One important remark should be made. Parameters of electronic components have a strong influence on the model predictions. Therefore, it is difficult to do the analysis without being sure that the schematics correspond to the actual hardware we used. Unfortunately, the situation with the FCAL'2003 beam test hardware is not very favorable in that sense. There is a number of private communications on possible modifications of the published schematics. A search for a solution based on guessing is not very productive. Therefore, the analysis described below is based on published documents only, in particular, on the description of the type IO-926 pre-amp found in [Ref. 2c].

3.2 The simulation model

The schematics used in the model are presented in Figures 16 and 17.

- The current generator **I1**, together with **L1, R6**, models the pulser operation;
- **R5** is the "injection R";
- **C1=Cpar** is a parasitic capacitance parallel to **R5**, defined by the SMD geometry and the printed circuit layout; it may vary between 0.5pF and 2pF (0.5 pF is "measured" in one channel, see Section 2.2);
- **R2** models a connection of the input cables: 0 – ***on***, ∞ – ***off***;
- **T1** is a pedestal cable;
- **R1** is the input cable impedance;
- **T2** is defined by the location of the pre-amplifier on the FEB board. By varying the **T2** delay, one can model the conductor between the FEB input pin and the pre-amplifier hybrid. The conductor length varies from 23 to 88 *mm* (0.15-0.6 *ns*);
- The hierarchical block **A_1** is the pre-amplifier (Fig. 17);
- The hierarchical block **S_1** describes the shaper: $\frac{s \cdot \tau}{(1 + s \cdot \tau)^3}$, $\tau = 13ns$, where s is a Laplace operator. The input impedance of the shaper is 50Ω.

With this model, let us take a look at the signal formation stages.

- **Input impedance and gain of the pre-amp** depend on frequency and, therefore, on signal development time. Fig. 18 shows the time evolution of parameters $|Z_{IN}|$ and G_I, following a step-like current function on the input. We see that <u>both parameters oscillate</u> before stabilizing in about 30 *ns*. The stable values depend on the input signal amplitude, with $|Z_{IN}|$ increasing by ~1.8% and G_I – by ~2.5% when the signal (DAC) rises from 500 to 5000. This means that even for slow input signals some non-linearity can be anticipated.

- **Input current in the pre-amplifier** (now with a pulser signal on the input). In Fig. 19 the waveforms of the pre-amplifier input current are shown for the pulser current *Ical* corresponding to DAC=500 and 5000. The waveforms are normalized to the *Ical* amplitudes to see deviations from linearity. For short input tracks and times beyond the transient phase, we get a practically linear behavior both with cables ***on*** and ***off*** (Fig. 19-1a,b). The same holds for long tracks with the cables ***on*** (Fig. 19-2a). The situation is sharply different for long tracks and cables ***off*** (Fig. 19-2b). A damping effect of the input cable is absent. The oscillations increase and last longer. The shape of the waveform becomes strongly dependent on the input amplitude, so one can expect a non-linearity to emerge.

- **Simulated output signals** are shown in Fig. 20. For a short input track the difference between low and high signals is small, respectively a non-linearity is small. For long input tracks and cables ***off*** we see a relative signal rise corresponding to an INL of 5%. A small table below shows the dependence on the parasitic capacitance **Cpar**:

Cpar, pF	0.5	1	2
$nonlin_R$, %	4	5	8

  In case of cables ***on***, the shaper output signal is insensitive to the input track length, and the non-linearity is small.[4]

- **The influence of the FEB location.** The model, presented in Fig 21,[5] gives the following result:

FEB#	**0**	**3**	**7**
$nonlin_R$, % , **Cpar**=1 pF	6.6	2.5	3
$nonlin_R$, %, **Cpar**=2 pF	10	2.5	6

  The positional dependence is due to an interference of reflected signals along the pulse bus. To be tested with an oscilloscope!
  So, in principle, the model does predict the difference between the FEBs. However, one has to assume a fairly large value for the parasitic capacitance **Cpar** to describe the observed trend (Fig. 9).

- **The influence of the calibration pulse shape (I1 current generator).** With a less steep rise-time and the shape closer to physical signals (for example, with TC1 tuned to 35 ns, see Fig. 16 for notations), the model for the cables ***off*** case predicts (Fig. 22) smaller the pre-amplifier current oscillations and a drop of the non-linearity down to the ~2% limit imposed by the G_I non-linearity. It should not be difficult to implement this feature in the real pulser.

We conclude that the model of Figures 16-17 predicts the ***on***|***off*** effects and can reproduce their typical magnitude and characteristic features (a dependence on the pre-amplifier location in a FEB and the difference between the FEBs). However, a few things remain to be rectified:

  - Whether or not the pre-amp schematics used for the model corresponds to a real FEB;[6]
  - Is the different behavior of the non-linearity in different FEBs entirely due to different FEB positions on the baseplane (the effect of parasitic capacitances), or partially due to different pre-amplifiers?

4. Concluding remarks

- ❖ One has to admit that the operation with disconnected input cables is not the regime which the amplifier had been designed for. Therefore, the observed off/on effects should not be regarded as a design problem.

- ❖ If the described interpretation of the observed ***on***|***off*** effects is valid, then "percentage-level" corrections involving pre-amplifier input impedance may not work, because the impedance is

[4] The values given here and in the next paragraph are quoted to DAC=500, with DAC(max)=5000.
[5] To be updated. This particular version of the model corresponds to an abstract case of a single FEB on the baseplane, with all other FEB slots having passive 12Ω plugs in. For convenience, the FEB is connected to a "FEB" block, not to a "slot", as it should be. The impedance of the input connecting track on the FEB is randomly chosen as 25Ω (to be verified; the FEB PCB documentation is needed).
[6] A visual inspection of pre-amplifier hybrids on two FEBs (Batch 215, July 1998) showed that the transistor Q3 of the pre-amp's white follower is not NE856, but 2SC4226. There were other (minor) discrepancies.

sensitive to the signal shape and a type of the input load.

- Still, **what the non-linearity is due to?**

Technically speaking, a large number of poles and feedback loops in the pre-amp (introduced to decrease power consumption) causes the impulse response function of the pre-amplifier to have an oscillatory character and be very sensitive to a presence of reactive elements on the input. Under ordinary working conditions, the oscillations are suppressed by a damping effect of the low-impedance input signal cables.

A critical role in the pre-amp schematics is played by a white-follower (Q2, Q3). It is derived from a usual emitter follower Q2 having a very non-linear response because of the special working regime, chosen to reduce power consumption. The linearity of the follower is restored by a deep feedback loop (Q3). The responsiveness of this feedback, very sensitive to the parameters (BF, TF) of transistors Q2 and Q3, is sufficient for the frequencies typical of physical signals from the calorimeter, but appears to fail for the pulser signals with a fast rise-time.

References

1. "Correction/Analysis of Calibration Data", a report by John Rutherfoord at the November'03 FCal meeting

2. Documentation of the FCal Beam Test'2003 electronics
a) "The LARG Calorimeter Calibration Board", J.Colas et al., ATL-LARG-2000-006
b) FCal baseplane design, BNL 10-981-1 Rev A, 8/28/02 KJW (a hardcopy obtained from F.Lanni)
c) "Preamplifier for the Liquid Argon Calorimeter", PRR April 26, 1999; FEB0 PCB layout: http://www.nevis.columbia.edu/~atlas/electronics/Module0FEB/Module0FEB.html
d) ATLAS Liquid Argon Caloribeter TDR, Section 10.4.2.2 (shaper design).

3. List of calibration runs used: the same as Sasha's

4."FCal Test Beam DAQ: description of raw data format", version 1.5, by P.Gorbunov http://atlas-fcaltb.web.cern.ch/atlas-fcaltb/Memos/index.htm

5. "A study of the calibration pulser behavior near DAC=0", V. Epshteyn and P.Gorbunov, ATLAS-FCAL beam tests 2003 Note 7, 2004-01-24, *in preparation*

Figures

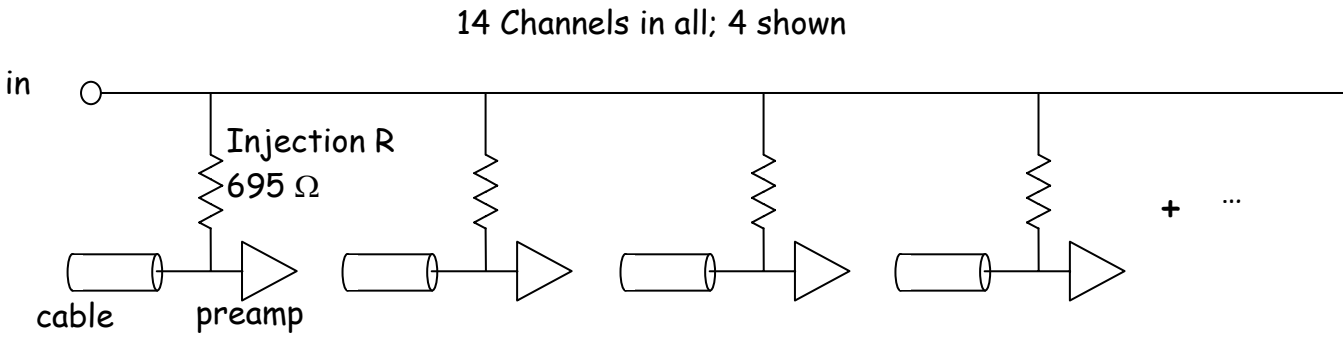

Fig.1 The electronic channel of the calibration pulser (from J.Rutherfoord's slides, Ref. [1]).

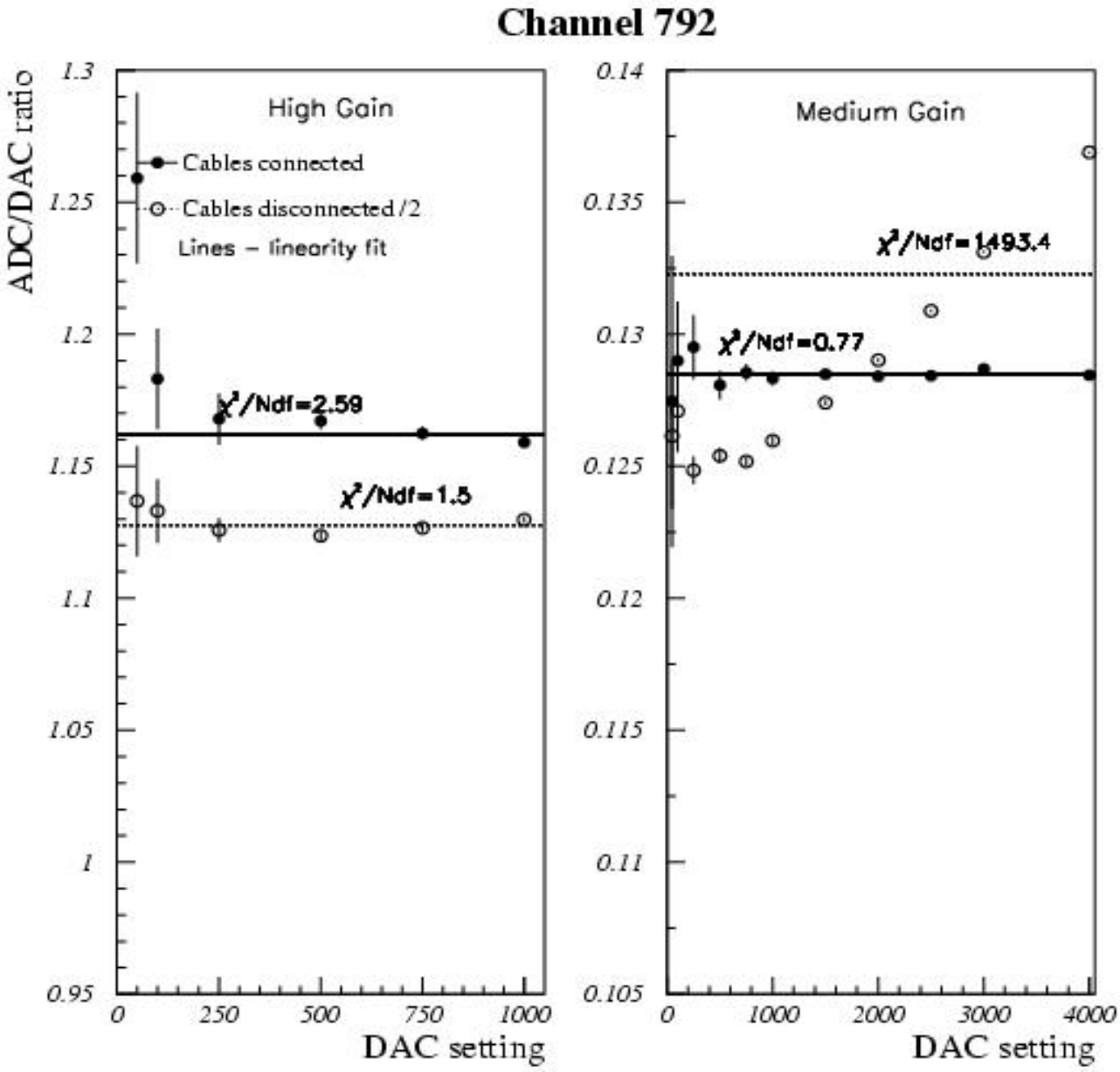

Fig. 2 The response of the electronic channel (from J.Rutherfoord's slides, Ref. [1]).

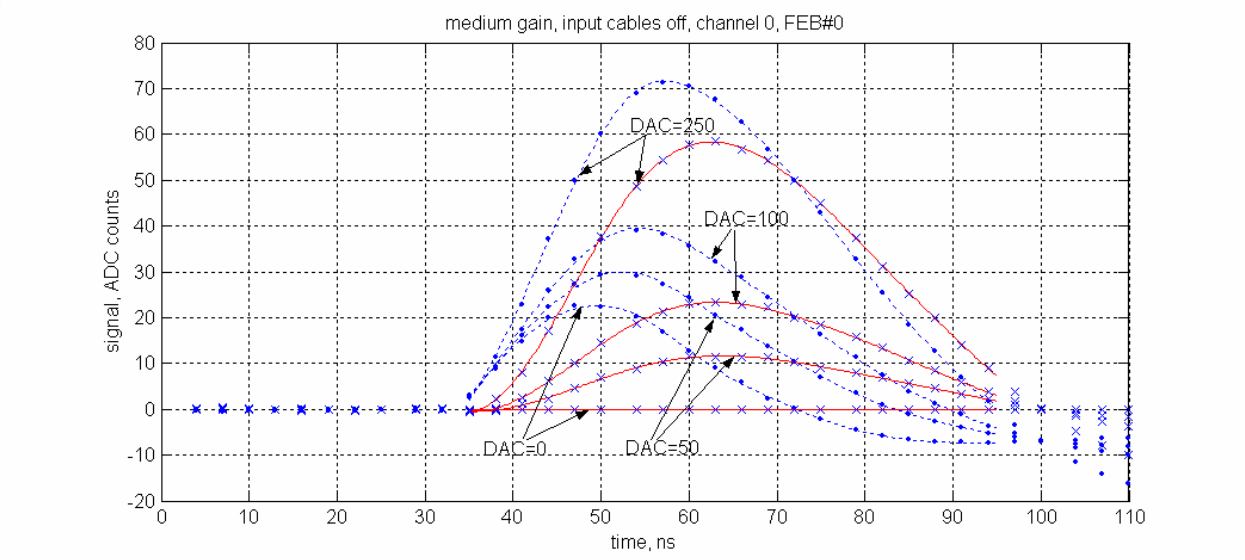

Fig. 3 Measured waveforms from calibration pulser runs (first 5 samples with different delays are shown).

… *raw values;* ××× the values after pedestal waveform subtraction*;* ___ *the waveform obtained by a fit with a 'cubic spline fit with smoothing'.*

.

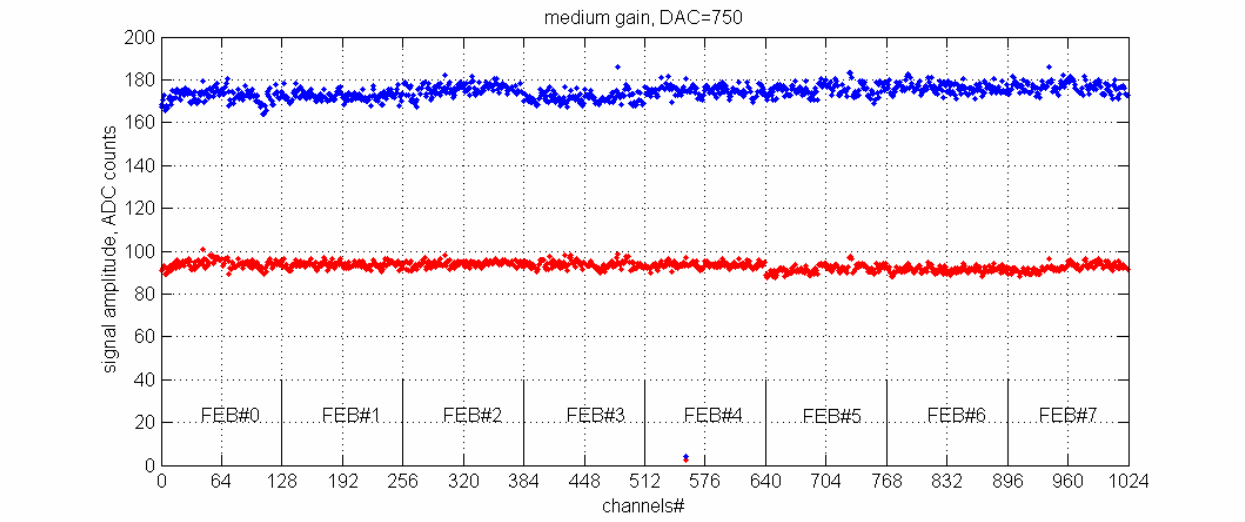

Fig. 4. The reconstructed calibration pulse amplitudes for DAC=750..
Input cables: **…** *- on,* **…**- *off.*

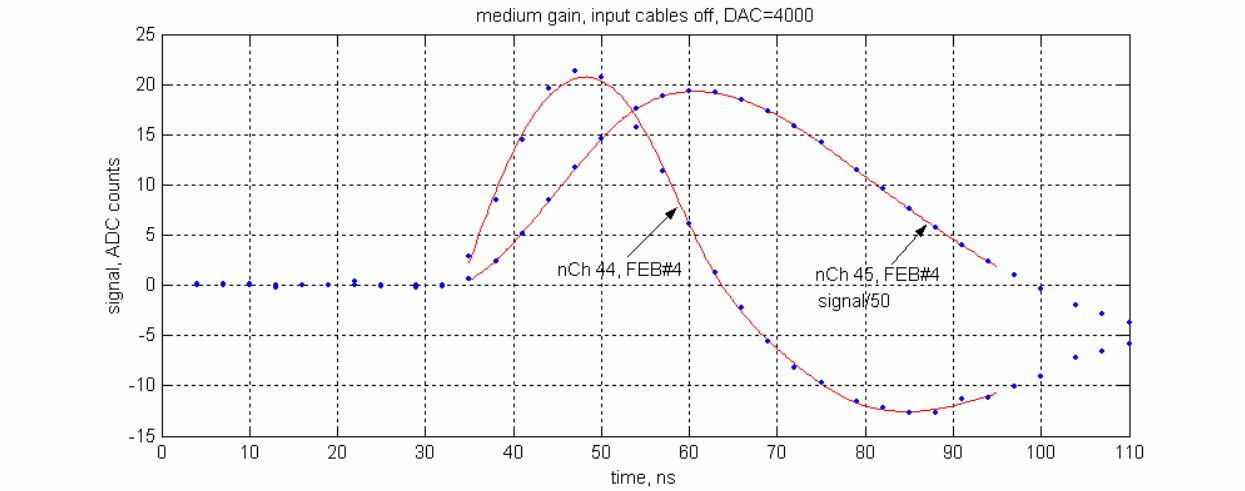

Fig. 5 A problem with Ch=44, FEB#4. The "broken" Ch. 44 is compared with a regular Ch. 45 (DAC=4000, medium gain, the Ch. 45 signal is divided by 50).

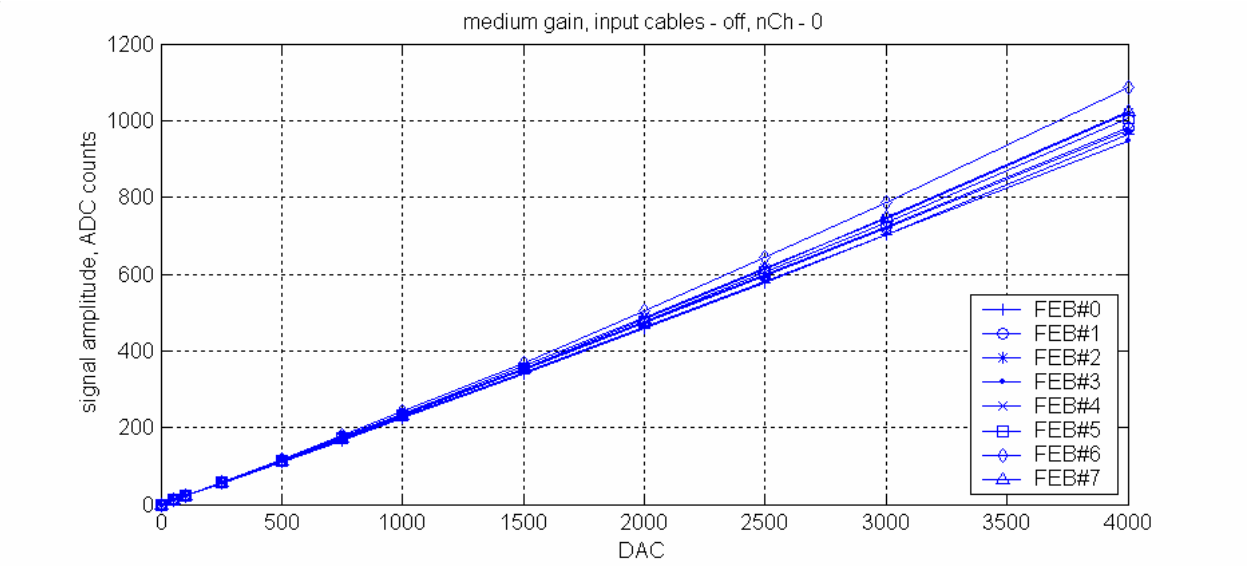

Fig. 6 An example of linearity scans in different FEBs.

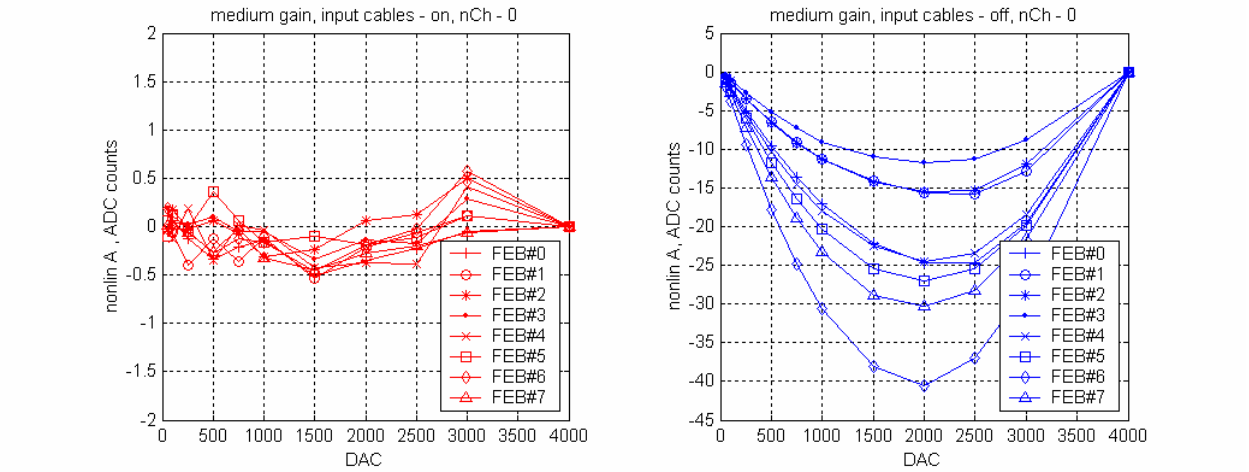

Fig. 7 An example of the measured non-linearity ($nonlin_A$), with input cables – on and off.

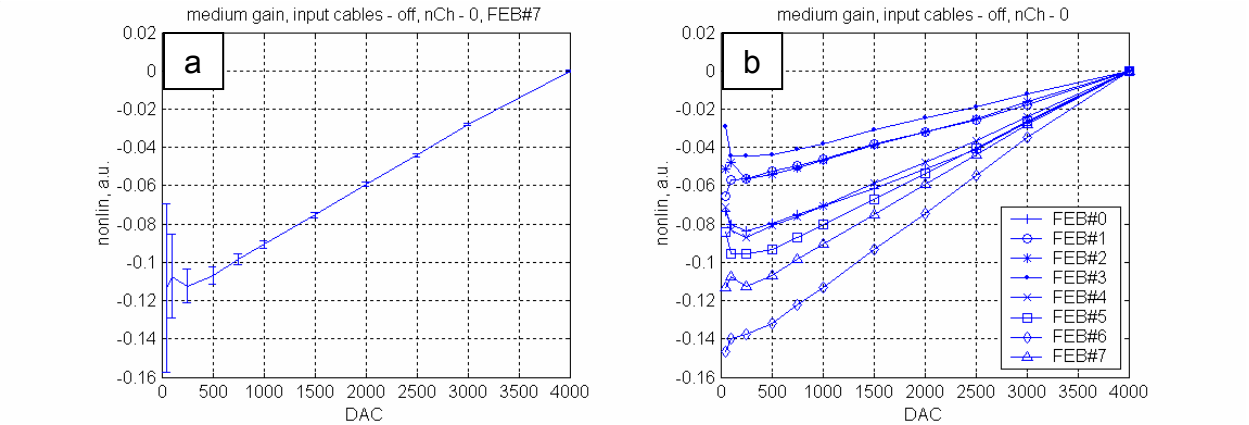

Fig.8. An example of measured relative non-linearity ($nonlin_R$),with input cables - off a – FEB# 7, b – FEB# 0-7. In (b) the errors are not shown, in order not to overload the picture.

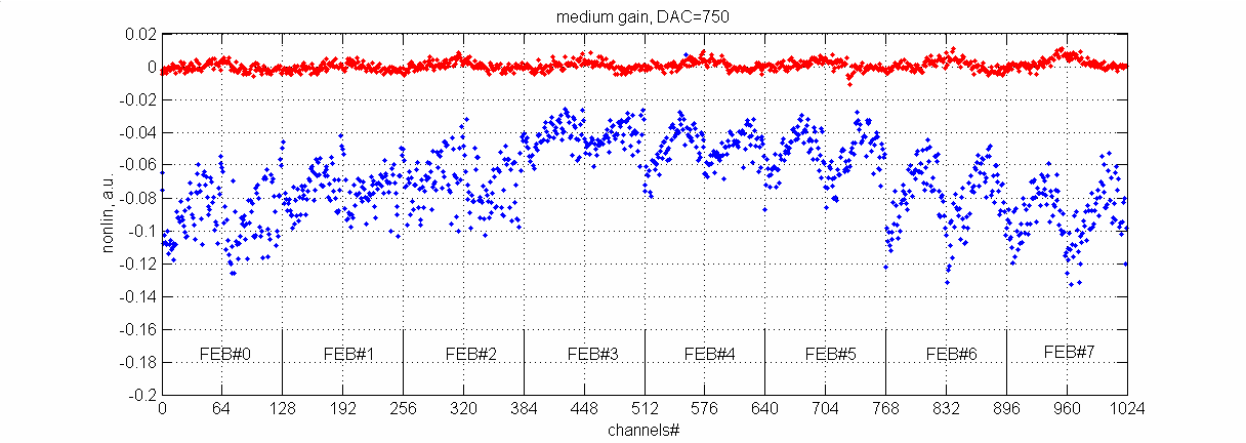

Fig. 9. A non-linearity in all calorimeter channels, for DAC=750, medium gain. Input cables: … – on, … - off

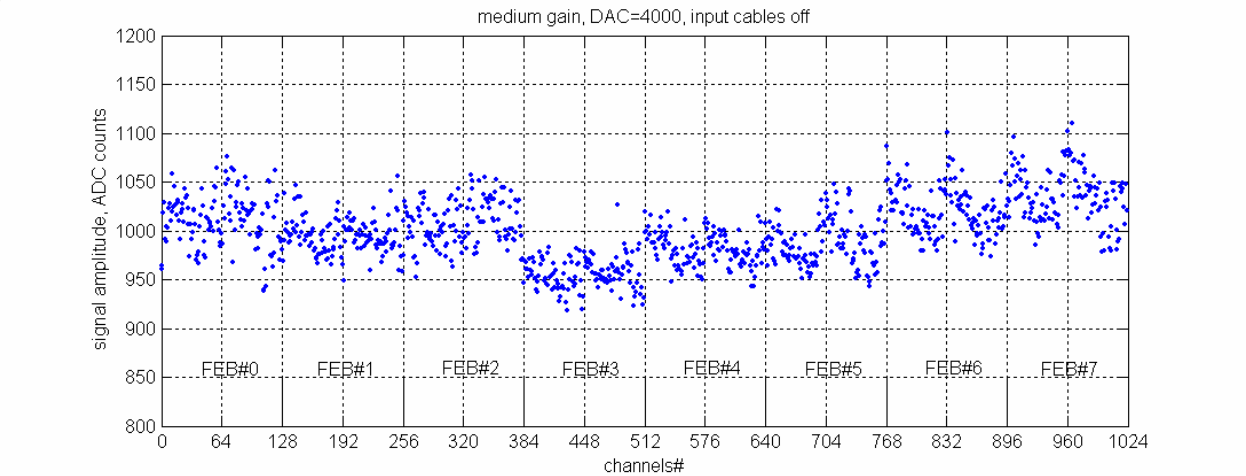

*Fig.10. Reconstructed signal amplitude for DAC=4000, cables **off**.*

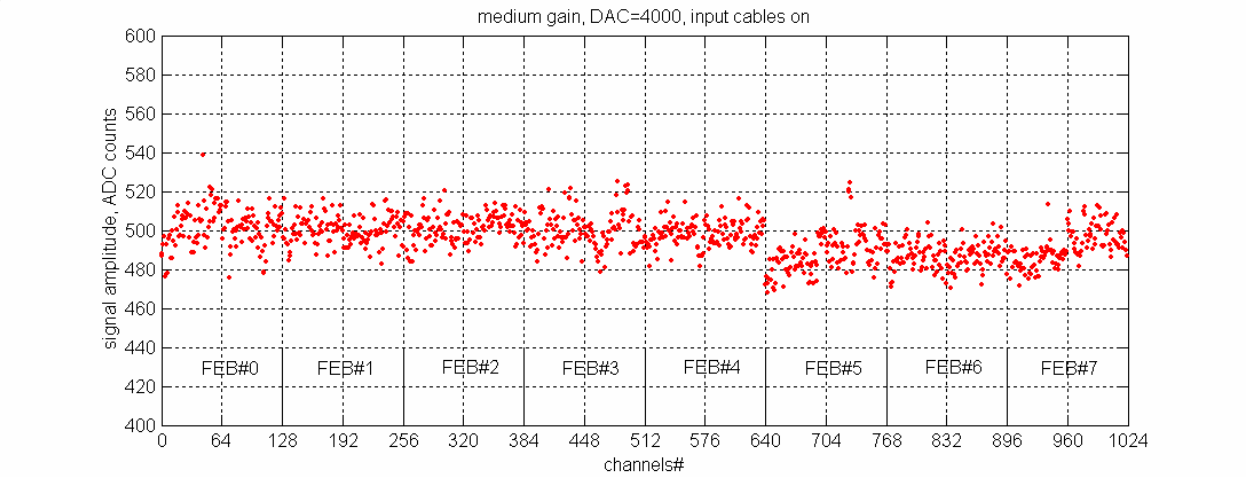

*Fig.11. Same Fig. 10, for input cables **on***

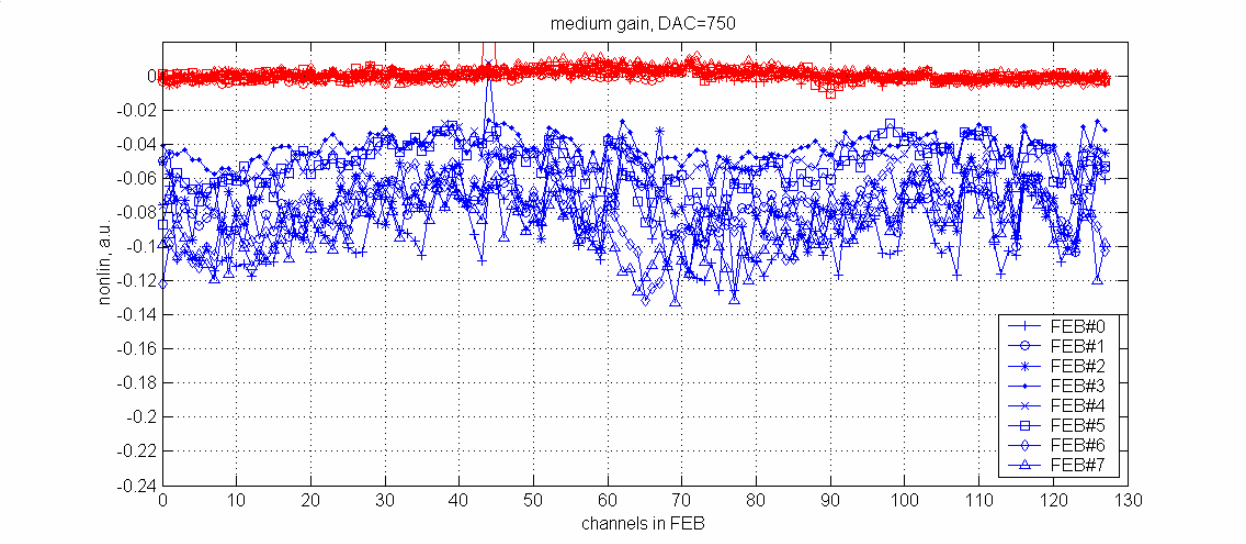

Fig. 12. A non-linearity as function of FEB input number (DAC=750, medium gain). Input cables: ___on, ___off

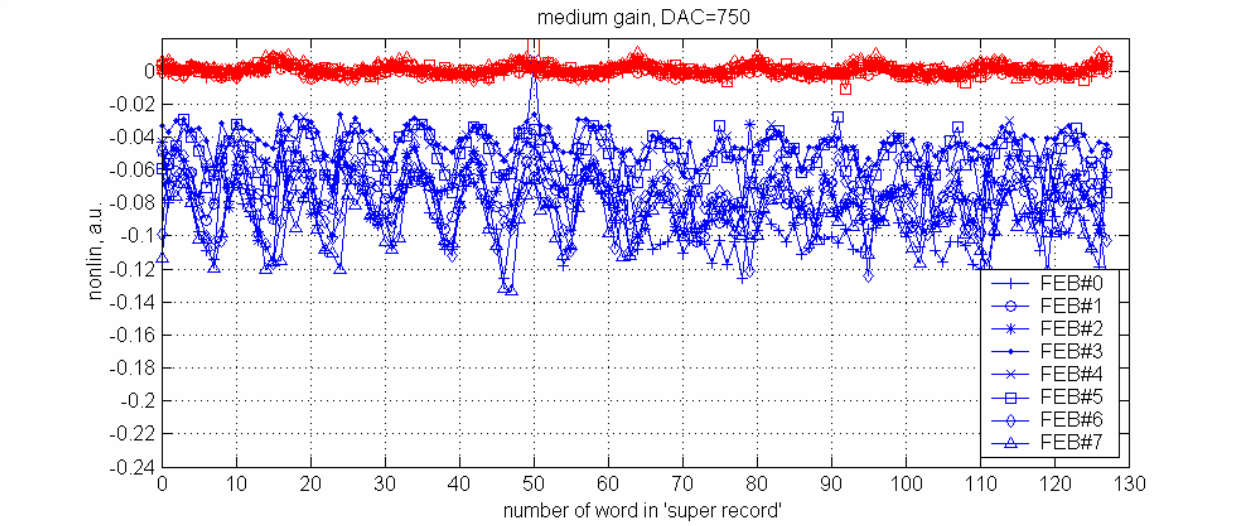

Fig.13. A non-linearity as function of a word number in a FEB data record (DAC=750, medium gain). Input cables: ___on, ___off

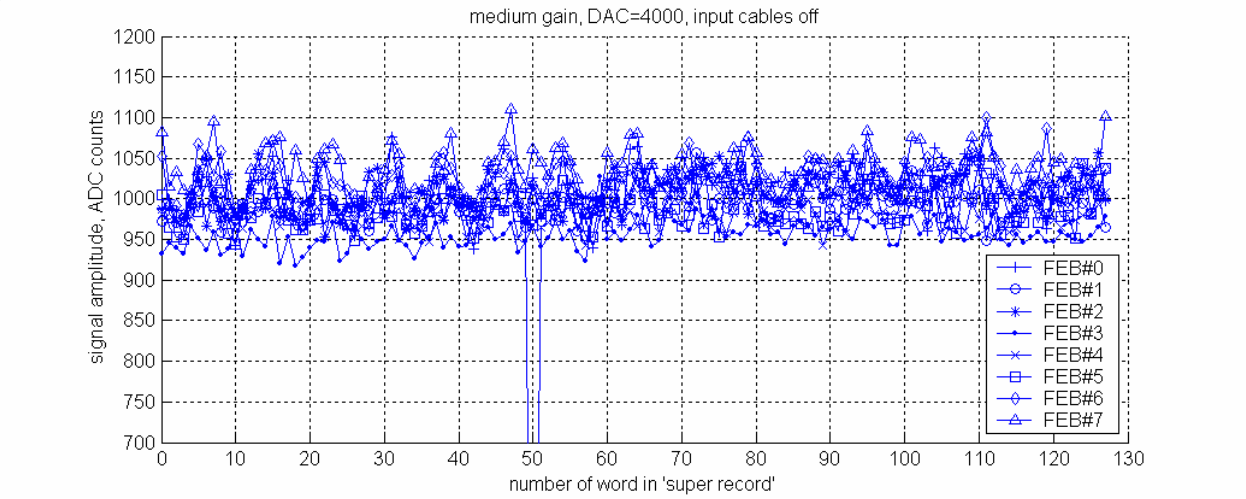

Fig. 14 Reconstructed signal amplitude for DAC=4000, as function of a word number in a FEB data record; cables off.

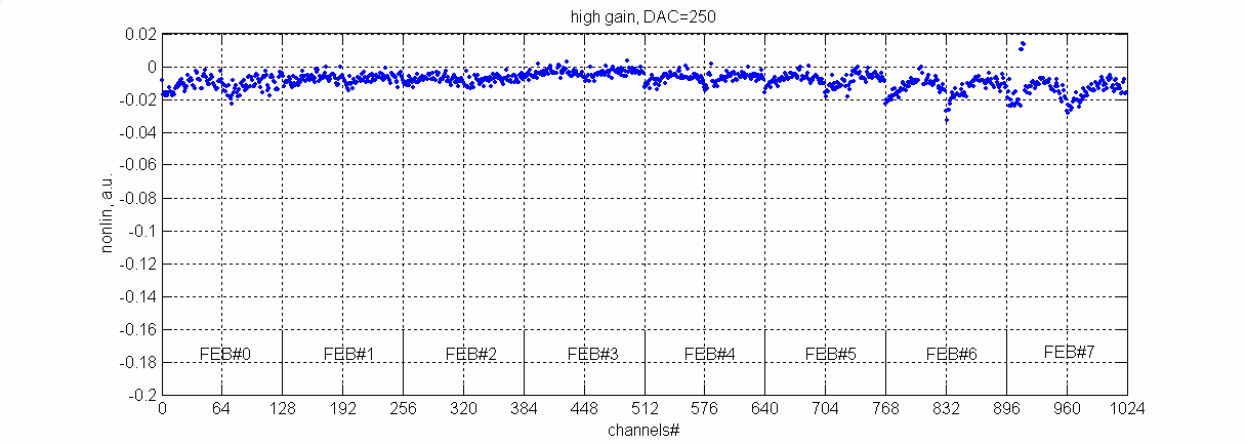

Fig .15. A non-linearity in all calorimeter channels, for DAC=250, high gain, input cables off.

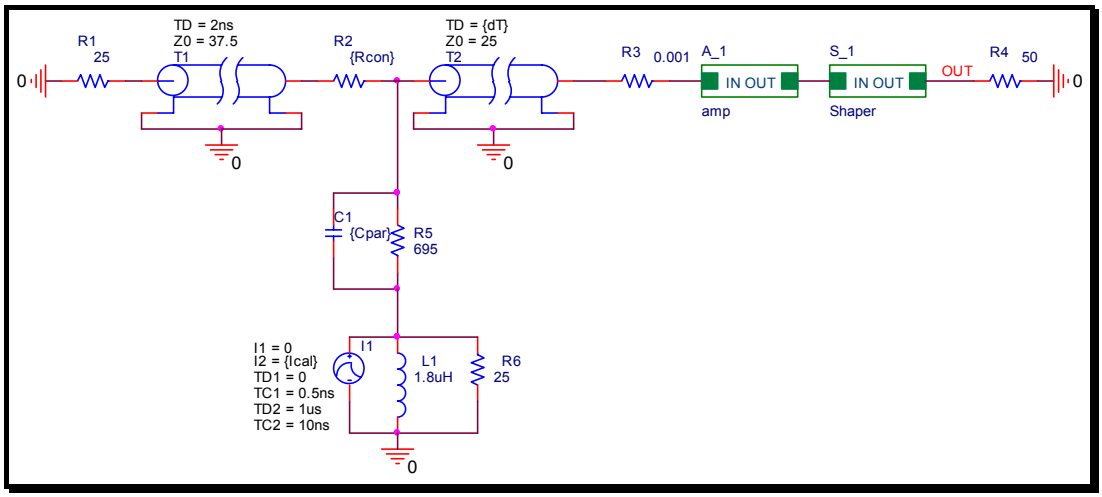

Fig. 16 A model used in the simulation.

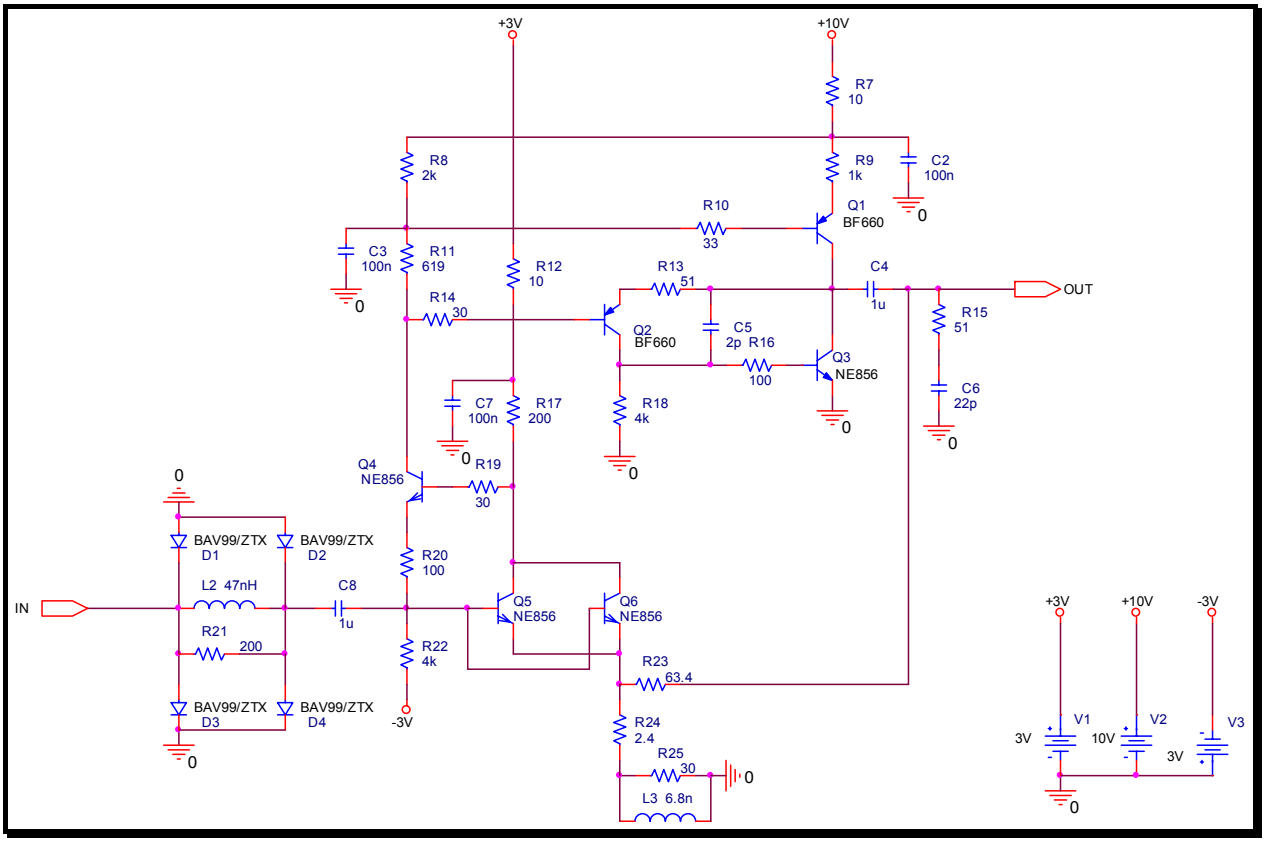

Fig.17. The circuit diagram of the pre-amplifier (Ref. [xxx]) used in the simulation.

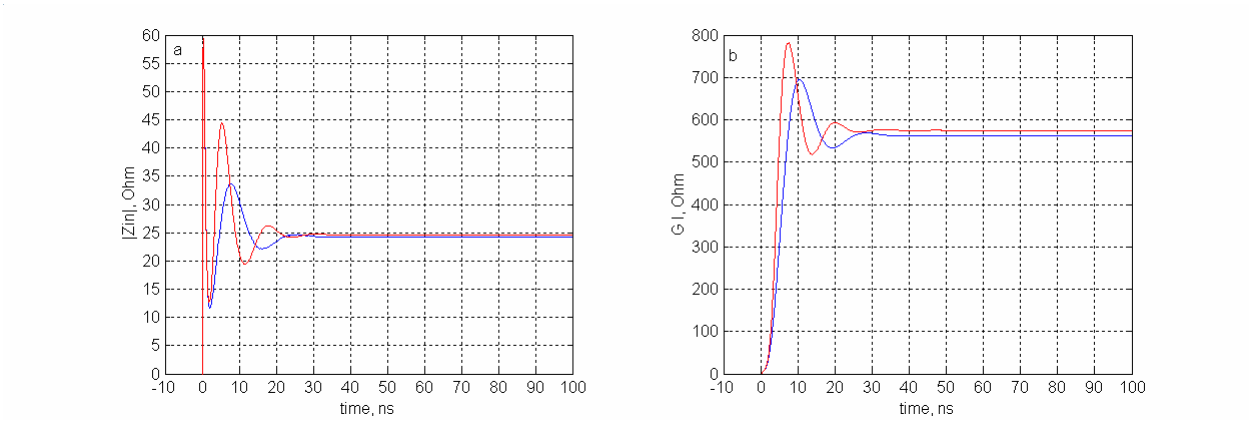

Fig.18. The input impedance (left) and the gain (right) of the pre-amplifier, as function of time, after a current step function applied on the input
The amplitude of the input current: ___DAC=500, ___DAC=5000

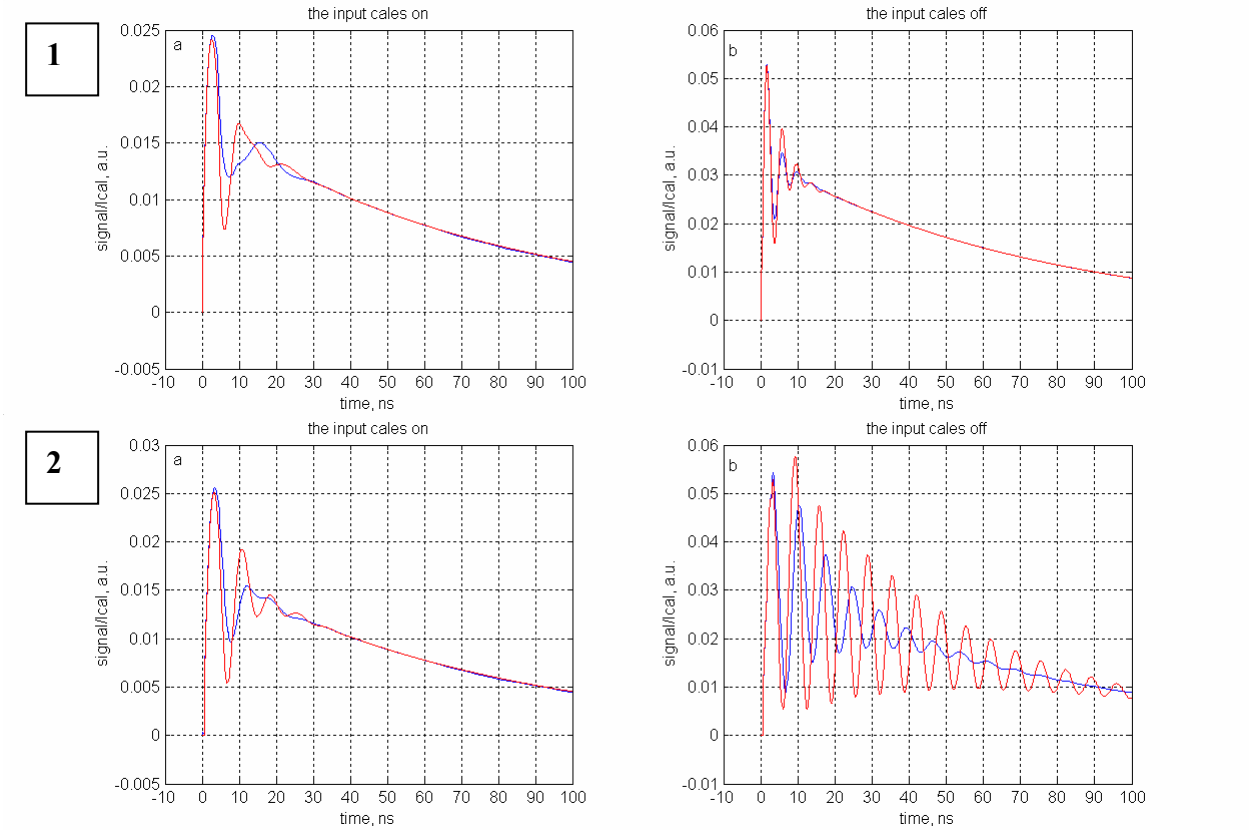

Fig .19. The pre-amp input current, Cpar=1pF
*track length: **1** - 23mm (dT=0.15ns), **2** – 88mm (dT=0.6ns)*
the input cables: a – on, b – off
Ical: ___500, ___5000,

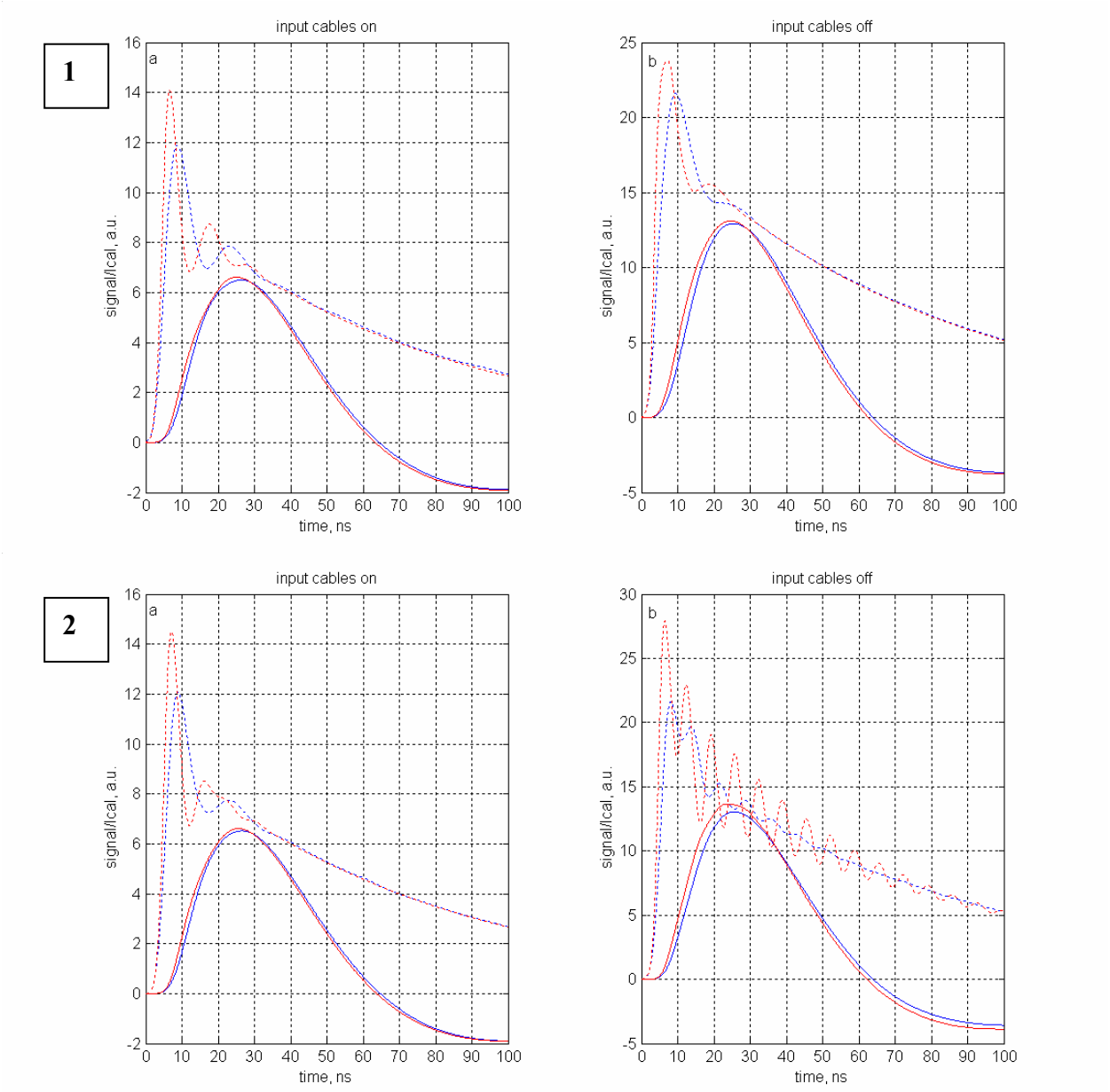

Fig. 20. Ouput signals from the pre-amplifier and the shaper, Cpar=1pF
*track length: **1** - 23mm (dT=0.15ns), **2** – 88mm (dT=0.6ns)*
the input cables: a – on, b – off
*Ical: ___500, ___5000, **…** after pre-amp, ___after shaper*

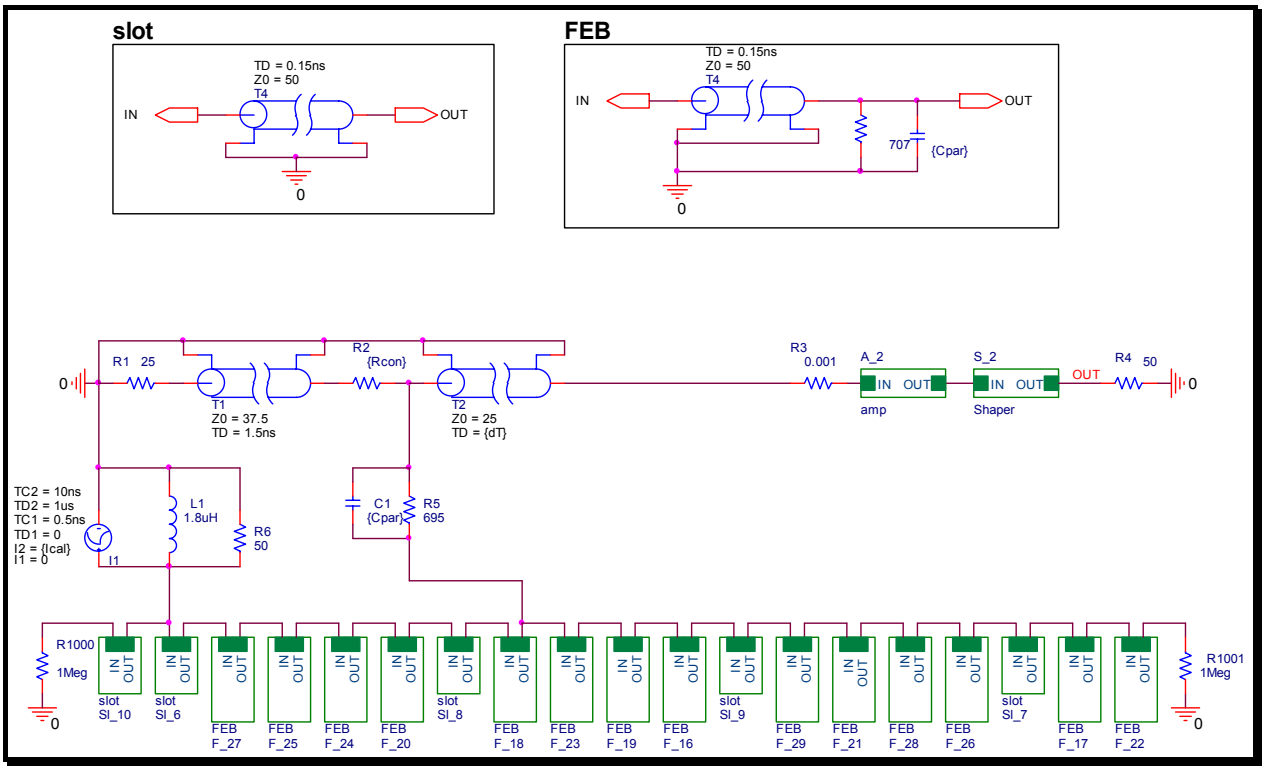

Fig .21. The model taking into account the FEB location in the crate

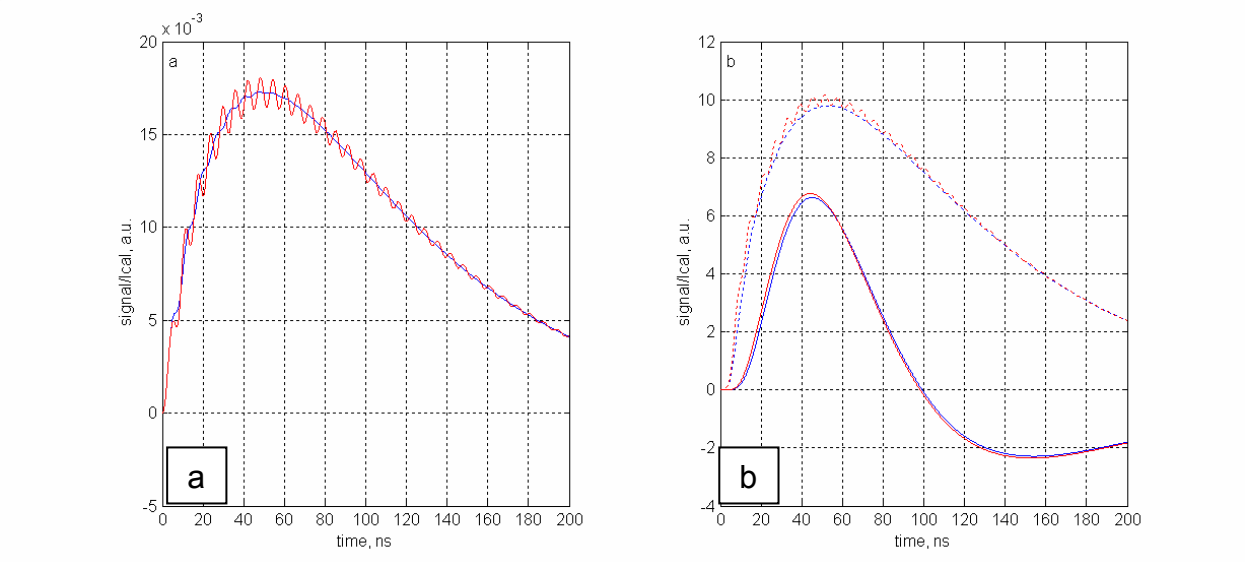

*Fig. 22. Signals in the pre-amplifier and shaper, with a calibration pulse shape similar to physical signals from the calorimeter, for input cables **off**. Cpar=1pF, track length=88 mm (dT=0.6 ns). a – input current of the pre-amplifier; b – output signals: **…** after pre-amp , ___ after shaper. Ical: ___500, ___5000,*